024 **SIMULATION AND EVALUATION OF ANISOTROPY ON 2D SHEAR WAVE ELASTOGRAPHY (SWE) IN A PHANTOM STUDY.**

*B. Jin, A. Evans, X. Zhou, S. Cochran, K. Skerl**
University of Dundee, Dundee, Scotland, UNITED KINGDOM.
Submitted for publication in final form: September 21, 2015.

Abstract: Anisotropy was observed in solid breast lesions during clinical application of Shear Wave Elastography (SWE). Hence, this project aims to investigate the correlation of the dimensions of the lesion on the anisotropy observed with SWE. Fifteen phantom lesions were developed; three silicone lesions, twelve regular shaped lesions and three irregular shaped lesions simulating benign and malignant in-vivo breast lesions. Our results suggest a correlation of anisotropy with lesion size, shape and stiffness in smaller lesions.

1. Background & Aims: Breast cancer is the most common cancer in women in the UK, one in eight women will be diagnosed with breast cancer during her life [1]. As breast cancer risk increases with age and to enable an earlier detection, women 50 years or older undergo a breast cancer screening using mammography in the UK. Mammography uses low-energy X-rays to image the human breast and hence has potential side effects [2]. Nevertheless, mammography is still the chosen method as it enables fast imaging and achieves a high sensitivity. However, only a low specificity is achieved. Hence, recalls of mammography are verified with ultrasound (US) imaging. US is especially used for women under 35 years old or in women with dense breasts [3]. Since 2009 SWE is added to the US examination to improve the benign/malignant differentiation [4, 5]. During the clinical application anisotropy, i.e. the directional dependence, of SWE values was observed [6]. Skerl et al. showed that malignant lesions are more anisotropic than benign lesions and anisotropy correlates with increasing stiffness [6]. However, solid breast lesions are rarely uniformly shaped and hence an influence by the lesion dimensions might be possible. Hence, this project aims to investigate the influence of the dimensions of the lesion on the anisotropy observed with SWE. Consequently, phantoms with lesions of different sizes, shapes and stiffness were developed.

Phantoms, i.e. artificial test objects, are commonly used for simulations in medical imaging. Various materials are established for different imaging modalities. US phantoms are often based on agar, gelatine or polyvinyl alcohol (PVA) [7]. The same materials are common for elastography imaging [8].

2. Methods:

2.1. Tofu phantom: First of all, we evaluated three lesions formed of commercial silicone. The silicone was placed on cling film and shaped into an ellipsoidal. Then the silicone lesions were left to dry for one week at air (Fig. 1). The dimensions of the three lesions used are 30x13x10 mm, 26x5x4 mm and 26x9x7 mm. The lesions were then positioned into tofu with a needle or the tofu was cut horizontally.

Fig. 1: One of the three silicon lesions used in this project

2.2. Agar based phantoms: Twelve agar based phantom lesions were developed in three breast tissue mimicking phantoms. The phantoms were made by using the recipe of Teirlinck et al. [9]. Nine of these lesions were regularly-shaped lesions (RL) whereas three were irregularly-shape (IL) simulating in-vivo breast lesions. Five RL and all three IL were made of a solution with 1.5% agar whereas the remaining four RL were made of a solution with 1.1% agar (size range 1-7.5 cm for all lesions). Agar-phantom 1 comprised five RL (lesions 1.1 – 1.5, 1.5% agar, Fig. 2a). Agar-phantom 2 comprised four RL (lesions 2.1 – 2.4, 1.1% agar, Fig. 2b). Lesions 1.1 – 1.4 and 2.1 – 2.4 were identical in their shape and size and differed only in their agar concentration. In addition lesions 1 – 4 were each identical in their shape but differed in size. Agar-phantom 3 comprised the IL (1.5% agar, Fig. 2c). The surrounding phantom material of all agar-phantoms had an agar concentration of 0.8%.

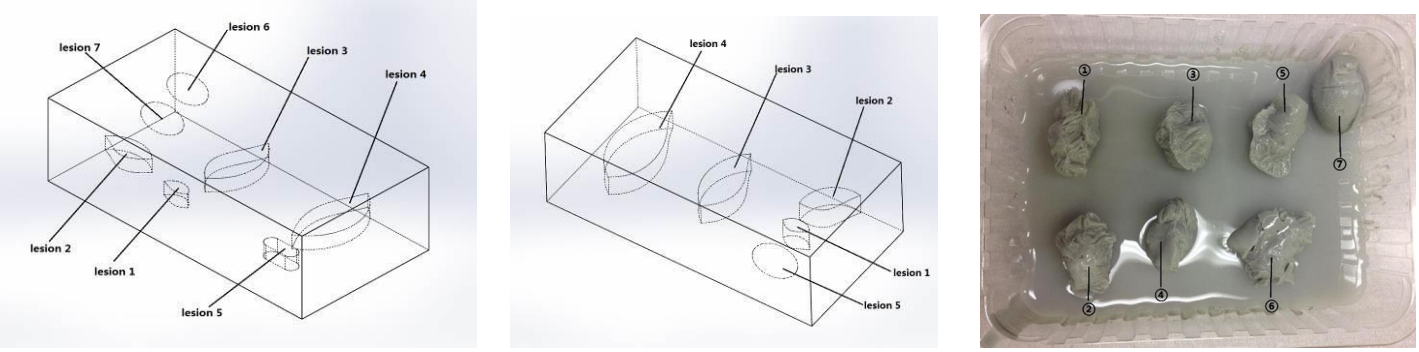

Fig. 2: Schemas of agar-phantom 1 (a), 2 (b) and 3 (c)

2.3. Ultrasound device: All images were observed using the ultrasound system Aixplorer (SuperSonic Imagine, Aix-en-Provence, France). The transducer had a frequency range of 7.5 to 15 MHz. The same probe was used to acquire the greyscale and SWE images.

2.4. Imaging process: All lesions were investigated in two orthogonal planes (along the long axis and along the short axis of the ellipsoidal) by four observers, two trained but unexperienced observers (KS, BJ) and two experienced observers (one radiologist (AE) and one radiographer (KT) both with an experience of more than 3 years in SWE imaging). Agar-phantom 3 was also investigated in two additional planes (45° and 135° to the long axis). Three images were performed for each imaging plane. The elasticity values maximum elasticity Emax, mean elasticity Emean and standard deviation SD were averaged and recorded for each image. We used Emean for the further evaluation and to calculate the anisotropic difference AD and the anisotropic factor AF of the averaged Emean values [6]:

$$AD = Long\ axis - Short\ axis, \quad AF = (Long\ axis - Short\ axis)^2$$

3. Results:

3.1. Tofu phantom: Two of the SWE images of the tofu phantom comprising three silicone lesions are shown in Fig. 3a-b. The silicone lesions are very hard and heterogeneous on SWE. Table 1 shows the measurements of them. All lesions are stiffer in the larger plane than in the shorter plane. However, a high SD value is observed. The AD and AF values differ between single lesions.

Table 1: SWE values of the three silicone lesions in the tofu phantom

Lesion	Axis	Emean [kPa]	Emax [kPa]	SD [kPa]	AD [kPa]	AF[kPa²]
1	Long	294	298	5.2	68	4556
	Short	226	283	33.4		
2	Long	163	215	38.6	7	44
	Short	156	191	22.9		
3	Long	213	241	17.2	140	19572
	Short	73	94	21		

Another tofu phantom was cut horizontally to insert the lesions. The SWE image is shown in Fig. 3c. No SWE values were estimated by the Aixplorer behind the cut.

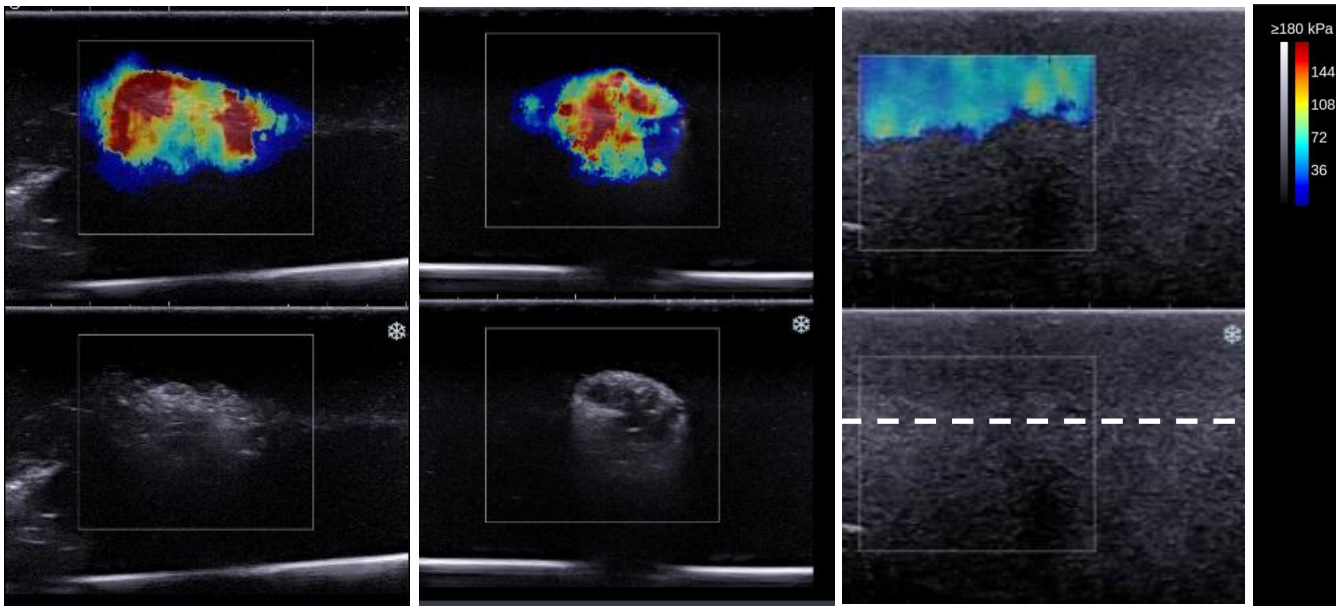

Fig. 3: a-b) SWE image of one of the three silicone lesions comprised in tofu. The silicone lesions are displayed as heterogeneous masses. c) SWE image of a cut tofu block. The white line overlaying the B-mode image indicates the cut. Although no cut is visible in the ultrasound image, no SWE values are displayed behind the cut.

3.2. Agar based phantoms: The averaged mean elasticity of the RL in agar-phantoms 1 and 2 are shown in Fig. 4.

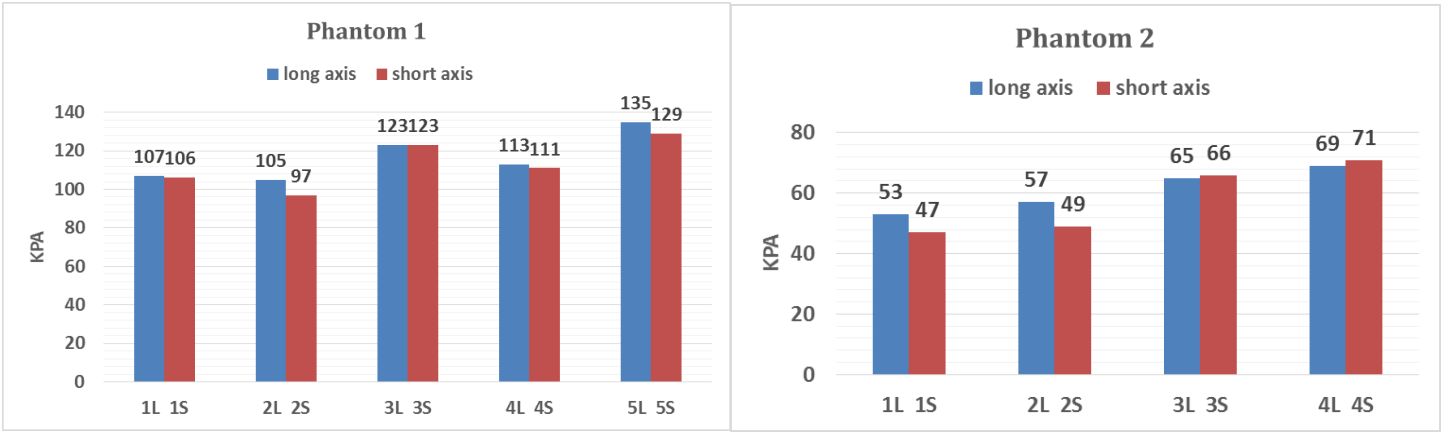

Fig. 4: Averaged mean elasticity values of the RL sorted by size in agar-phantoms 1 and 2. All long axes of RL in agar-phantom 1 are stiffer or equal as the short axes. However, in agar-phantom 2 only the long axes of lesions 2-1 and 2-2 are stiffer whereas the short axes of the other two RL are stiffer.

AD and AF depend on the agar concentration in the smaller lesions 2-1, 1-2, and 2-2 but not in the larger lesions (Fig. 5).

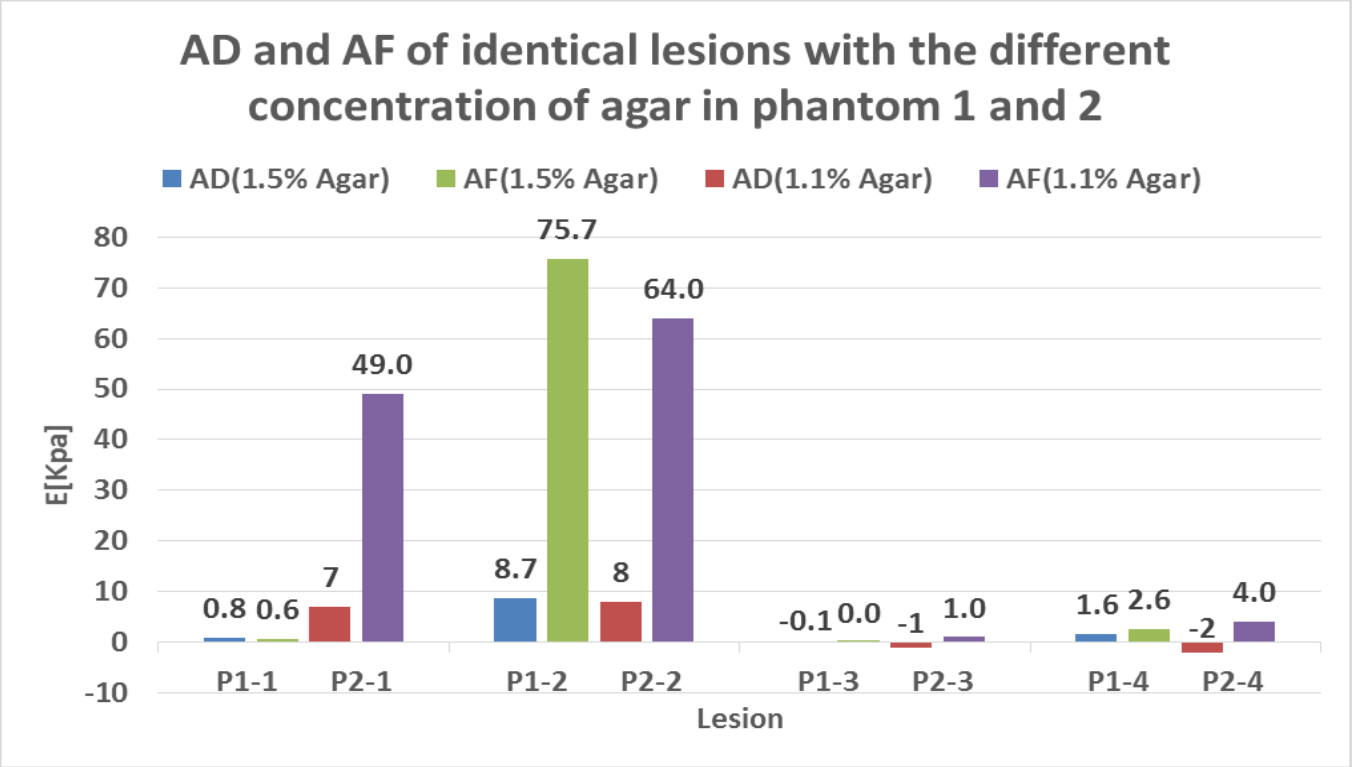

Figure 5: AD and AF of lesions identical in shape and size with a different agar concentration (agar-phantoms 1 and 2). They differ in the smaller lesions (2-1, 1-2, and 2-2) but not in the larger ones (1-3, 2-3, 1-4, and 2-4).

AD of the additional two orthogonal planes in agar-phantom 3 comprising IL equals the AD of the long and short axes (Table 2). Especially in lesions 3-2 all Emean values equal each other.

Lesion	Imaging plane			
	0°	45°	90°	135°
3-1	102	89	93	99
3-2	107	105	108	101
3-3	110	98	103	125

Table 2: Emean values in the four imaging planes of the IL in agar-phantom 3 (0°, 45°, 90°, 135°). The AD of two orthogonal planes is similar independent of the direction.

4. Conclusions: Our results suggest that anisotropy correlates with the lesion dimensions in smaller lesions (diameter<5 mm) but not in larger lesions. In addition anisotropy of smaller lesions correlates with the stiffness of the lesion. Anisotropy is also influenced by the shape of the lesion (regular vs. irregular). However, the anisotropy observed in this phantom study is inferior to the anisotropy observed in in-vivo solid breast lesions [6]. This suggests that in-vivo interactions with the surrounding tissue influence anisotropy observed on SWE. This hypothesis is supported by the observations of Skerl et al. showing an increased anisotropy in malignant lesions and in invasive cancers [6].

We have also shown that tofu and silicone are only limited suitable for SWE experiments. The main issue with tofu is the ability to insert lesions as shear waves seem not to be able to propagate through cut tofu. Silicone on the other hand creates a very heterogeneous stiffness pattern if dried on air. However, this might be advantage when simulating malignant tissues as malignant tissues are heterogeneous in their structure and on SWE [5]. Due to these results, we developed our further phantoms using an agar solution. This material achieves a more homogeneous mass. However, its stiffness reproducibility and homogeneity is questionable as contents like silicone powder sink to the bottom when poured into the mould. As the stiffness in PVA phantoms is created by several freeze-thaw cycles [8], PVA might enable a more homogeneous and reproducible elasticity. PVA phantoms have to undergo about three freeze-thaw cycles to achieve the stiffness of healthy tissue and even more often to mimic cancerous tissue [10]. However, this procedure is also more time consuming and could hence not be used during this limited project.

We performed our measurements with four different observers. Each measurement was performed three times by each observer and the results were averaged for their evaluation. This might have biased the results as outliners influenced the results. In addition we observed a partly high inter-observer variability which might also have biased our results.

Hence, further investigations would be of interest. These investigations might help to clarify in more detail correlations between anisotropy observed on SWE and the tissue subtype and structure.

References:

[1] Olson, J. *Bathsheba's breast: Women, cancer, and history*. JHU Press, 2002.

[2] Dixon, J.*ABC of breast diseases*. Vol. 69. John Wiley & Sons, 2009.

[3] Hindle, W, Davis, L et al. Clinical value of mammography for symptomatic women 35 years of age and younger. *American journal of obstetrics and gynecology,* 180.6 : 1484-1490, 1999.

[4] Berg, W., Cosgrove, D. et al. Shear-wave elastography improves the specificity of breast US: the BE1 multinational study of 939 masses. *Radiology, 262*(2), 435-449, 2012. doi: 10.1148/radiol.11110640

[5] Evans, A., Whelehan, P. et al. Quantitative shear wave ultrasound elastography: initial experience in solid breast masses. *Breast Cancer Research: BCR, 12*(6), R104-R104, 2010. doi: 10.1186/bcr2787

[6] Skerl, K., Vinnicombe, S. et al. Anisotropy in solid breast lesions at shear wave elastography: relationship to the radial plane and implications for benign/malignant differentiation. Oral presentation at the annual meeting of B*reast Cancer Research , November 2013, Liverpool.*

[7] Madsen, E., Hobson, M. et al. "Tissue-mimicking agar/gelatin materials for use in heterogeneous elastography phantoms."*Physics in medicine and biology,* 50.23: 5597, 2005.

[8] Fromageau, J., Brusseau, E. et al. "Characterization of PVA cryogel for intravascular ultrasound elasticity imaging."*Ultrasonics, Ferroelectrics, and Frequency Control, IEEE Transactions on*50.10 (2003): 1318-1324.

[9] Teirlinck, C., Bezemer, R. et al. Development of an example flow test object and comparison of five of these test objects, constructed in various laboratories. *Ultrasonics, 36*(1-5), 653-660, 1998.

[10] Cournane, S., Cannon, L. et al. Assessment of the accuracy of an ultrasound elastography liver scanning system using a PVA-cryogel phantom with optimal acoustic and mechanical properties. *Physics in medicine and biology*55.19: 5965, 2010.